Supporting Information

Si/SiO$_x$ Hollow Nanospheres/Nitrogen-Doped Carbon Superstructure with Double Shell and Void for High-Rate and Long-Life Lithium-Ion Storage

Chao Yang,[ab] Yelong Zhang,[a] Jinhui Zhou,[a] Chunfu Lin,[b] Fan Lv,[a] Kai Wang,[a] Jianrui Feng,[a] Zhikun Xu,[c] Jianbao Li,[b] and Shaojun Guo*[a]

[a]Department of Materials Science and Engineering, College of Engineering, Peking University, Beijing 100871, China. *E-mail: guosj@pku.edu.cn

[b]State Key Laboratory of Marine Resource Utilization in South China Sea, Key Laboratory of Ministry of Education for Advanced Materials in Tropical Island Resources, College of Materials and Chemical Engineering, Hainan University, Haikou 570228, Hainan, PR China

[c]Key Laboratory for Photonic and Electronic Bandgap Materials, Ministry of Education, School of Physics and Electronic Engineering, Harbin Normal University, Harbin 150025, Heilongjiang, P. R. China

Figures

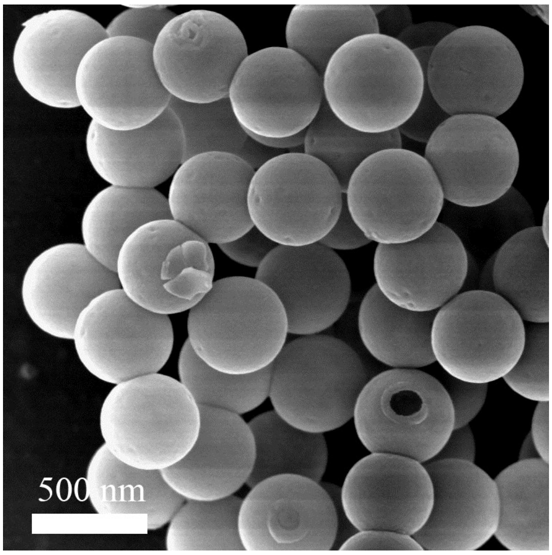

Fig. S1 SEM image of SiO_2 hollow nanospheres with an average diameter of ~450 nm.

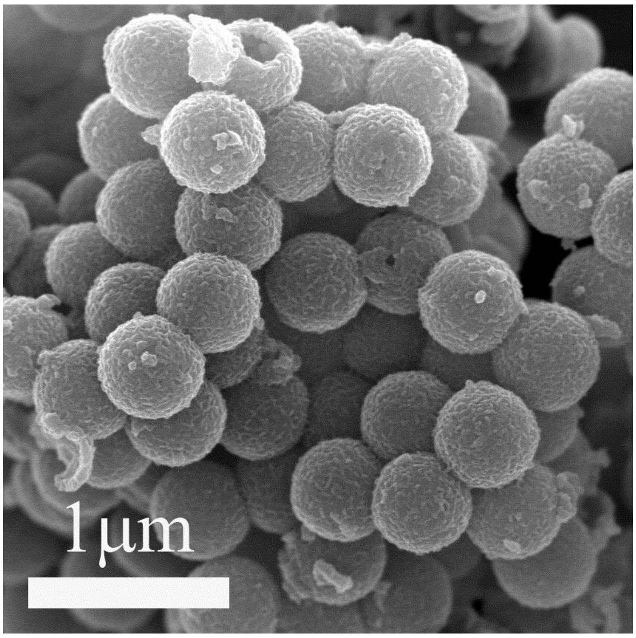

Fig. S2 SEM image of Si/SiO_x-DSHSs.

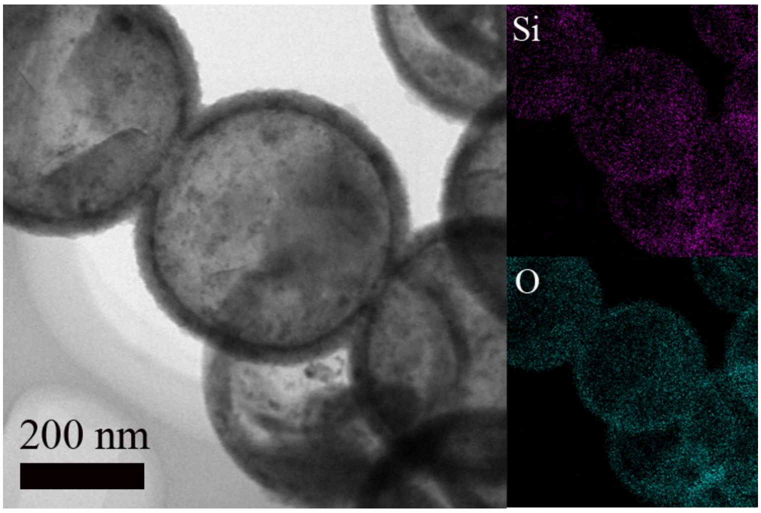

Fig. S3 TEM image of Si/SiO_2 and its corresponding EDS elemental mapping.

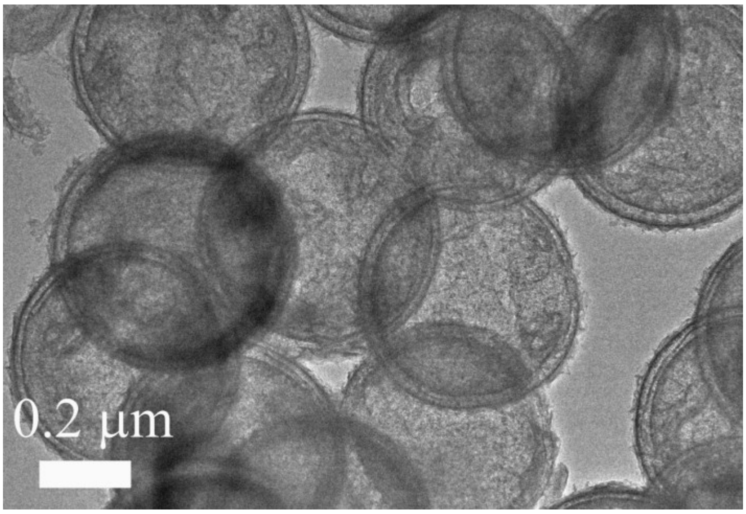

Fig. S4 Low magnification TEM image of Si/SiO$_x$-DSHSs.

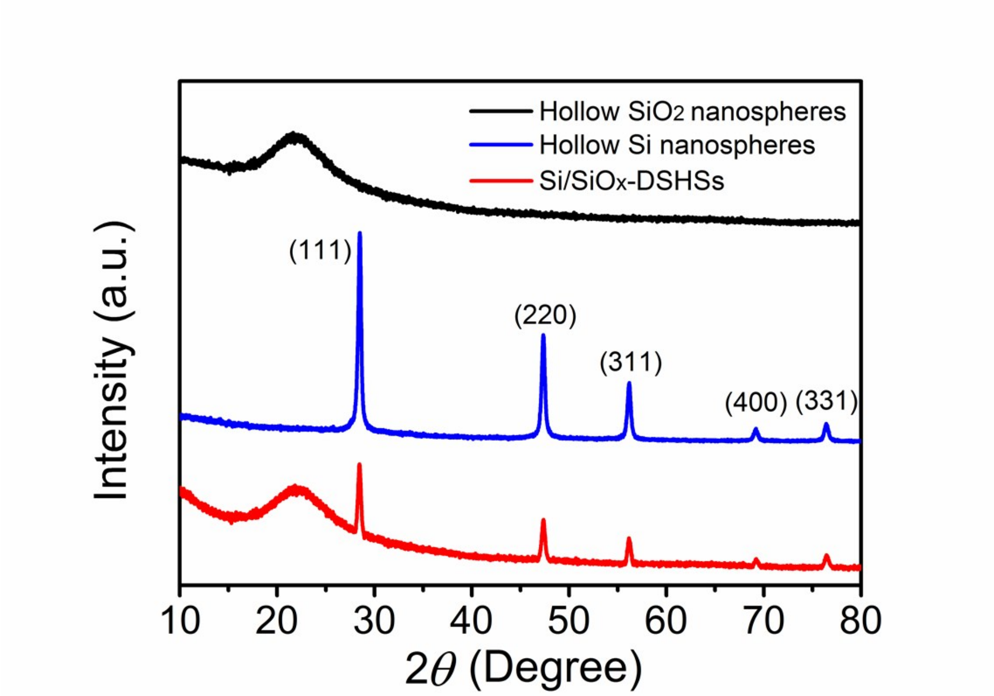

Fig. S5 XRD patterns of Si hollow nanospheres, SiO$_2$ hollow nanospheres and Si/SiO$_x$-DSHSs.

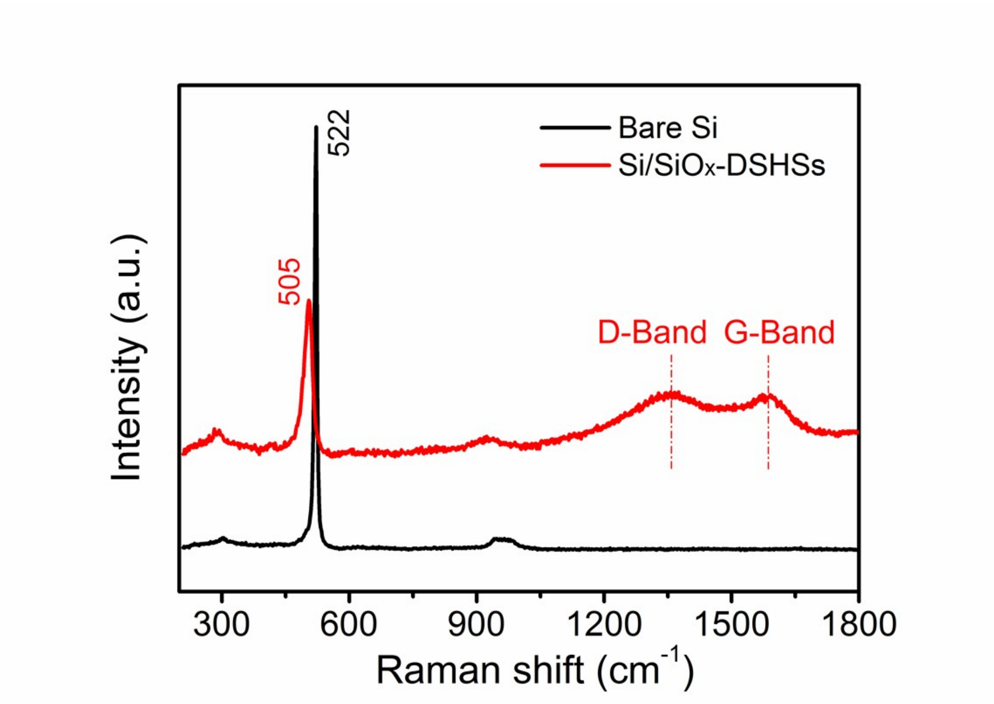

Fig. S6 Raman spectra of the bare Si and Si/SiO_x-DSHSs.

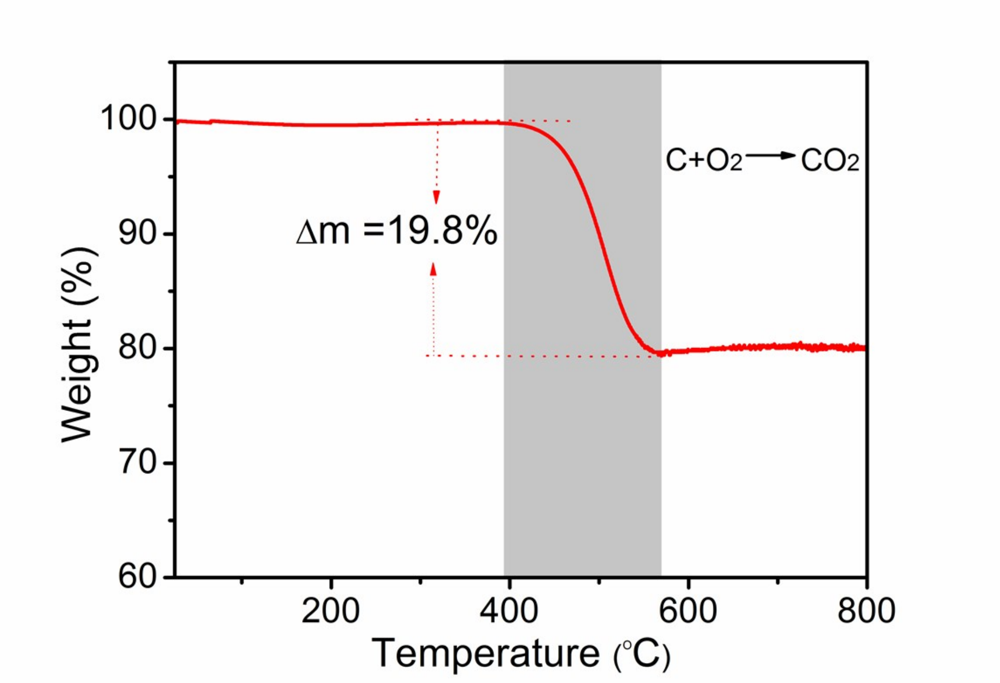

Fig. S7 Thermogravimetric analysis curve of the Si/SiO_x-DSHSs.

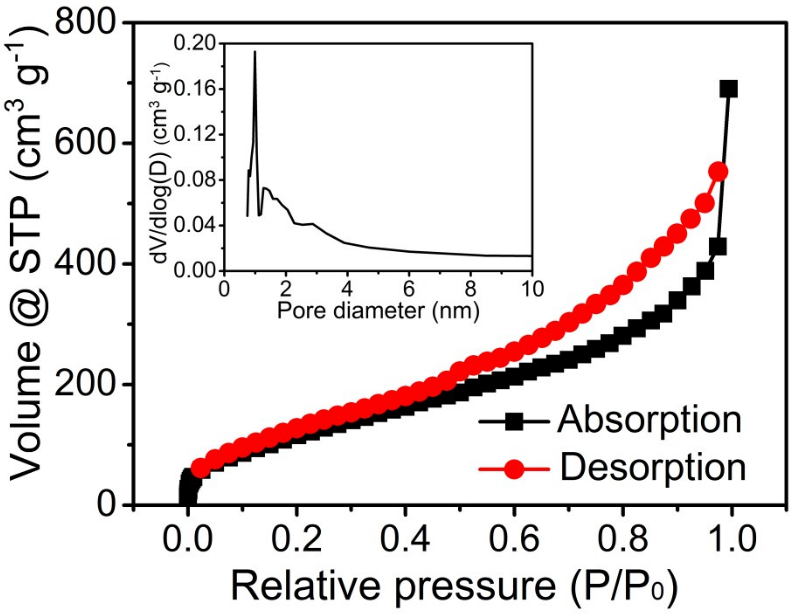

Fig. S8 Nitrogen adsorption and desorption isotherm of the Si/SiO_x-DSHSs alongside its porosity information.

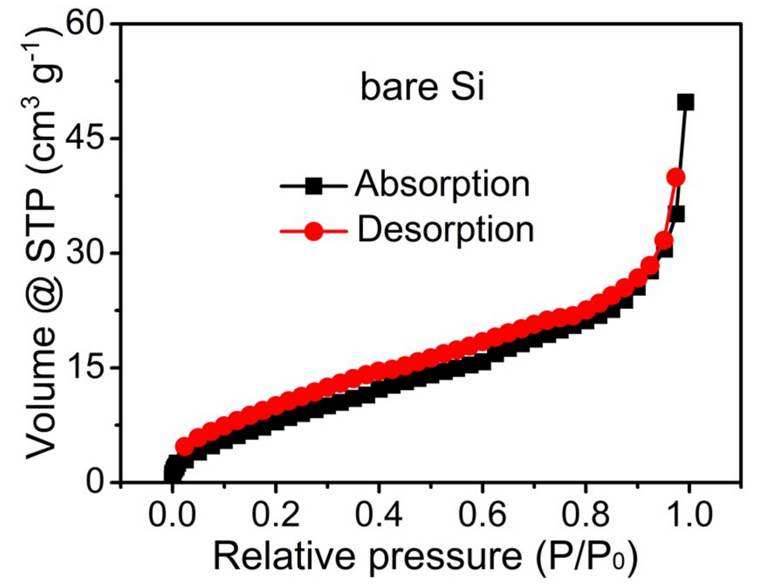

Fig. S9 N_2 adsorption–desorption isotherm of commercial Si nanoparticles.

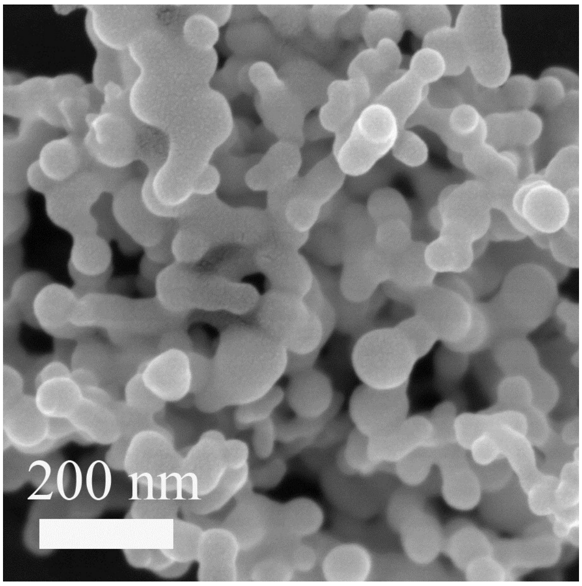

Fig. S10 The SEM images of commercial Si nanoparticles with an average size of ~70 nm.

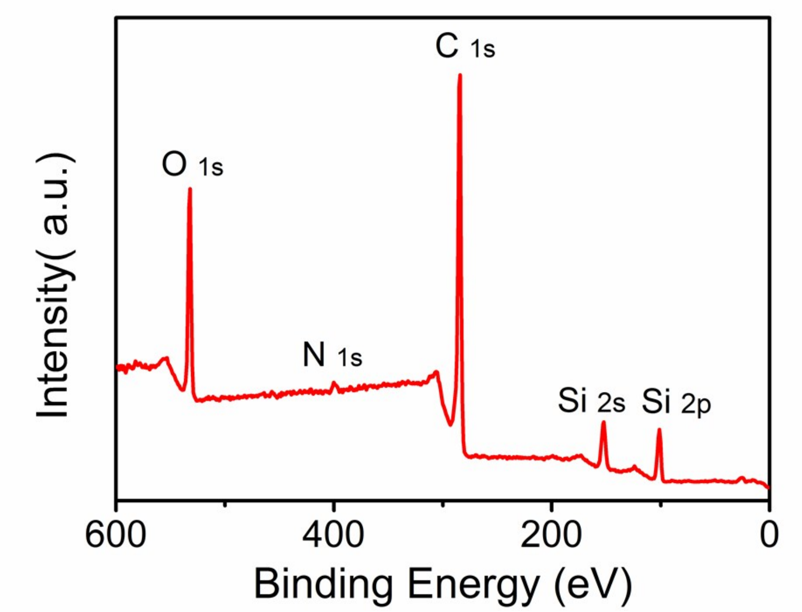

Fig. S11 Survey XPS spectra of as-prepared Si/SiO_x-DSHSs.

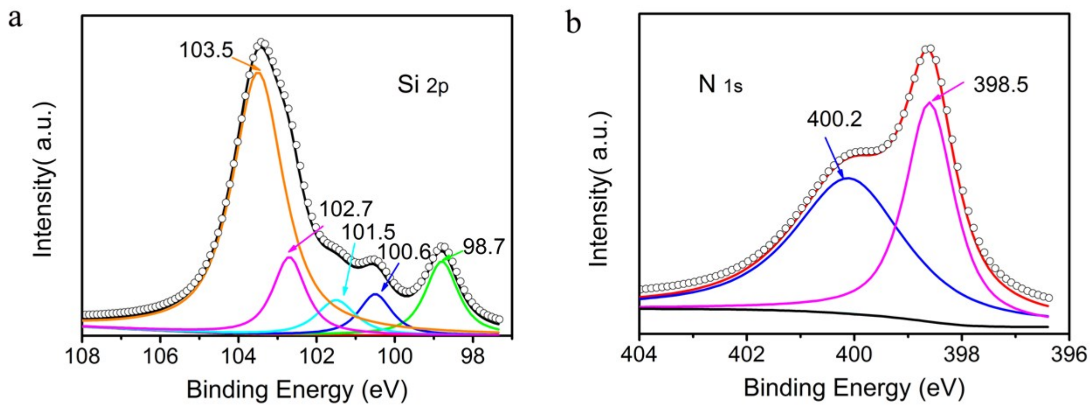

Fig. S12 XPS spectra of the Si/SiO$_x$-DSHSs (a) Si 2p signal and (b) N 1s signal.

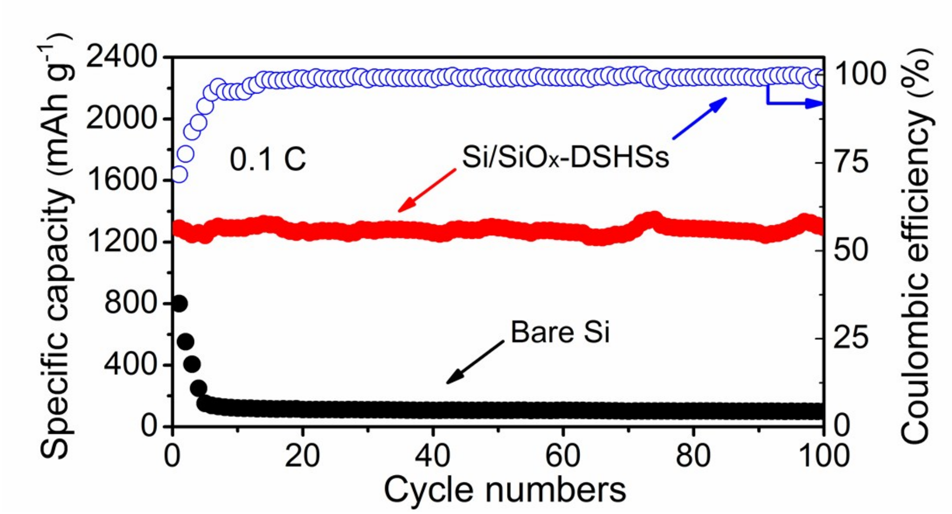

Fig. S13 The cycling performance of bare Si and Si/SiO$_x$-DSHSs electrodes for 100 cycles at 0.1 C.

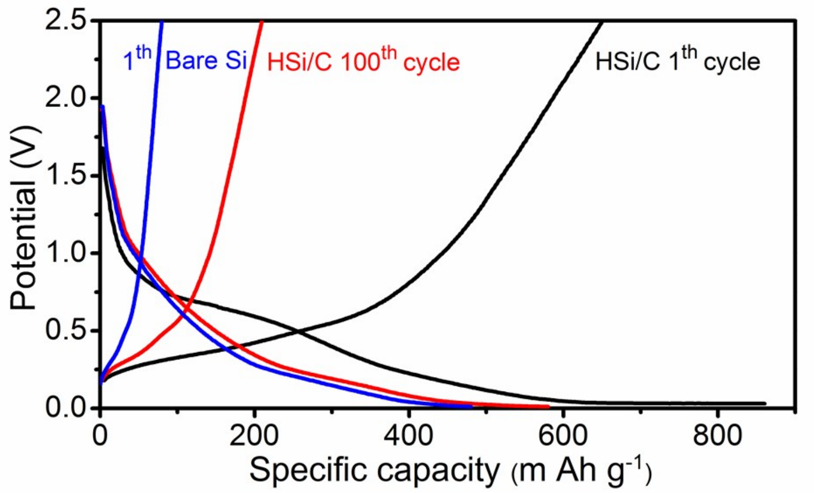

Fig. S14 Charging/discharging profiles of bare Si and carbon coated hollow Si nanosphere (HSi/C) electrodes at different cycles at a high current rate of 5 C.

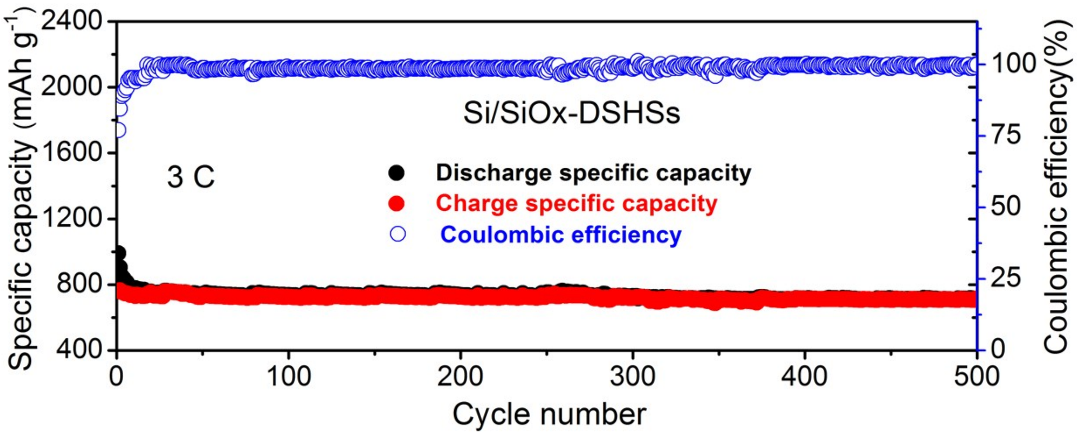

Fig. S15 The cycling performance of Si/SiO_x-DSHSs electrodes for 500 cycles at 3 C with a reversible capacity of around 750 mAh g^{-1} and an excellent cycle retention of 94.5% after 500 cycles.

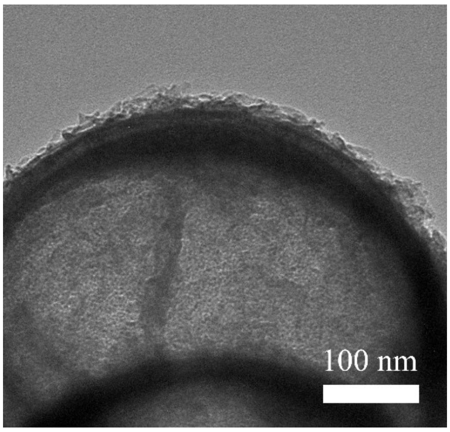

Fig. S16 TEM image of cycled Si/SiO_x-DSHSs electrode, showing structural integrity of carbon shell and thin SEI layer.

Table S1 Comparison of electrochemical properties of Si/SiO_x-DSHSs with previously reported Si-based anode materials. Electrode compositions are listed using mass ratios of active material : conductive carbon : binder.

Material	Electrode composition	Loading density (mg cm^{-2})	Rate capability	Cycling performance	Initial CE	Reference
Si/SiO_x-DSHSs	70 : 20 : 10	1.5	1290, 1203, 1160, 1005, 750, 562 and 360 mA h g^{-1} at 0.1, 0.2, 0.5, 1, 3, 5 and 10 C, respectively	1231 mA h g^{-1} after 100 cycles 0.1 C 709 mA h g^{-1} after 500 cycles 3 C 323 mA h g^{-1} after 1000 cycles at 10 C	71.7%	this work
Carbon-Coated Silicon/Graphite Spherical Composites	65 : 25 : 10	1.4	700 mA h g^{-1} at 2 C;	568 mA h g^{-1} after 100 cycles 0.2 C 500 mA h g^{-1} after 100 cycles 1 C	–	S1

Yolk-shell silicon-mesoporous carbon	80 : 15 : 5	–	–	999.8 mA h g^{-1} after 400 cycles 0.42 A g^{-1}	–	S2
Porous Si Nanowires	70 : 20 : 10	1.0	548 mA h g^{-1}; 282 mA h g^{-1} at 7.2 A g^{-1}	1503 mA h g^{-1} after 560 cycles 0.6 A g^{-1}	43%	S3
3D microfibers constructed from silicon–carbon	75 : 15 : 10	–	500 mA h g^{-1} at 2 C	860 mA h g^{-1} after 200 cycles 0.3 C	–	S4
Si/N-doped carbon/CNT spheres	70 : 20 : 10	1.1–1.4	978 mA h g^{-1} at 1 A g^{-1}	1031 mA h g^{-1} after 100 cycles 0.5 A g^{-1}	72%	S5
Silicon-Reduced Graphene Oxide	70 : 20 : 10	0.2	–	778 mA h g^{-1} after 100 cycles 50 mA g^{-1}	–	S6
Crystalline-Amorphous Core-Shell Silicon Nanowires	70 : 20 : 10	–	–	1060 mA h g^{-1} after 100 cycles 0.85 A g^{-1}	–	S7
Si/Reduced Graphene Oxide Bilayer Nanomembranes	70 : 20 : 10	–	636, 325, 111 mA h g^{-1} at 3, 7, and 15 A g^{-1}, respectively	821 mA h g^{-1} after700 cycles1 A g^{-1} 571 mA h g^{-1} after 2000 cycles 3 A g^{-1}	59%1 A g^{-1} 48%3 A g^{-1}	S8
Silicon embedded in porous carbon matrix	70 : 20 : 10	–	~1000, 750 mA h g^{-1} at 5 and 10 A g^{-1}, respectively	736 mA h g^{-1} after 800 cycles 2 A g^{-1}	–	S9

Table S2 Impedance parameters and Li^+-ion diffusion coefficients of Bare Si, cycled cell of bare Si and Si/SiO_x-DSHSs.

Sample	R_b (Ω)	R_1 (Ω)	R_2 (Ω)	σ (Ω $s^{-0.5}$)	D (cm^2 s^{-1})
Fresh of bare Si	2.24	-	150.3	64.9	4.57×10^{-12}
Cycled cell of bare Si	3.79	-	231.6	-	-
Si/SiO_x-DSHSs	2.33	35.6	30.7	6.83	8.69×10^{-11}

The calculation of Li^+-ion diffusion coefficient

The Li^+-ion diffusion coefficients of Si/SiO_x-DSHSs and bare Si can be calculated according to the following equations:[S10]

$$Z' = R_b + R_1 + R_2 + \sigma\omega^{-1/2} \quad \text{(S1)}$$

$$D = R^2T^2 / (2S^2F^4C^2\sigma^2) \quad \text{(S2)}$$

where R_b, Z', ω, R, T, S, F and C refer to the Ohmic resistance of the half cell, the real part of the impedance, the angular frequency in the low-frequency region, the gas constant, the absolute temperature, the real surface area, the Faraday constant and the molar Li^+-ion concentration, respectively; R_1 and CPE_1 in the equivalent electrode circuit model (the *inset* of Fig. 3a) refer to the Li^+-ion desolvation/adsorption and electron transfer; R_2 and CPE_2 are associated with Li^+-ion insertion in the particle surface; σ represents the Warburg factor, which is relative to Z'–$\omega^{-1/2}$ (Equation (S1)) and can be obtained by measuring the slope of the oblique line in the low-frequency region (Fig. 3b).

References

[S1] S. Y. Kim, J. Lee, B.-H. Kim, Y.-J. Kim, K. S. Yang and M.-S. Park, *ACS Appl. Mater. Interfaces*, 2016, **8**, 12109.

[S2] W. Luo,Y. X. Wang, S. L. Chou, Y. F. Xu, W. Li, B. Kong, S. X. Dou, H. K. Liu and J. P. Yang, *Nano Energy*, 2016, **27**, 255.

[S3] Y. Chen, L. F. Liu, J. Xiong, T. Z. Yang,Y. Qin and C. L. Yan, *Adv. Funct. Mater.*, 2015, **25**, 6701.

[S4] C. F. Zhang, R. X. Yu, T. F. Zhou, Z. X. Chen, H. K. Liu and Z. P. Guo, *Carbon*, 2014, **72**, 169.

[S5] Y.-C. Zhang, Y. You, S. Xin, Y.-X. Yin, J. Zhang, P. Wang, X.-S. Zheng, F.-F. Cao and Y.-G. Guo, *Nano Energy*, 2016, **25**, 120.

[S6] G. Ferraresi, L. Czornomaz, C. Villevieille, P. Novák and M. E. Kazzi, *ACS Appl. Mater. Interfaces*, 2016, **8**, 29791.

[S7] L.-F. Cui, R. Ruffo, C. K. Chan, H. L. Peng and Y. Cui, *Nano Lett.*, 2009, **9**, 491.

[S8] X. H. Liu, J. Zhang, W. P. Si, L. X. Xi, B. Eichler, C. L. Yan and O. G. Schmidt, *ACS Nano*, 2015, **9**, 1198.

[S9] C. B. Liao, Q. K. Xu, C. Wu, D. L. Fang, S. Y. Chen, S. M. Chen, J. S. Luo and L. Li, *J. Mater. Chem. A*, 2016, **4**, 17215.

[S10] C. Yang, S. Yu, C. F. Lin, F. Lv, S. Q. Wu, Y. Yang, W. Wang, Z.-Z. Zhu, J. B. Li, N. Wang and S. J. Guo, *ACS Nano*, 2017, **11**, 4217.